



Performance analysis of multi-GNSS PPP for accurate ship-borne positioning in Antarctic region

Volkan Özbey ^{*1}, Bilal Mutlu ¹, Serdar Erol ¹, Mahmut Oğuz Selbesoğlu ¹, Hasan Hakan Yavaşoğlu ¹, Reha Metin Alkan ¹

¹ Istanbul Technical University, Geomatics Engineering Department, Türkiye, ozbeyv@itu.edu.tr, mutlubil@itu.edu.tr, erol@itu.edu.tr, selbesoglu@itu.edu.tr, yavasoglu@itu.edu.tr, alkanr@itu.edu.tr

Cite this study:

Özbey, V., Mutlu, B., Erol, S., Selbesoğlu, M. O., Yavaşoğlu, H. H., & Alkan, R. M. (2025). Performance analysis of multi-GNSS PPP for accurate ship-borne positioning in Antarctic region. *International Journal of Engineering and Geosciences*, 10(3), 428-439.

<https://doi.org/10.26833/ijeg.1574964>

Keywords

Precise Point Positioning
Marine Surveying
Antarctica
PRIDE PPP-AR
Ginan

Research Article

Received:26.11.2024
1.Revised: 31.01.2025
2.Revised: 27.02.2025
Accepted:18.03.2025
Published:01.10.2025



Abstract

This study evaluates the performance of multi-constellation GNSS Precise Point Positioning (PPP) for offshore kinematic observations in the challenging environment of Antarctica using the data collected on a moving ship during the 6th Turkish Antarctic Expedition in 2022. The analysis involved two open-source PPP software solutions, PRIDE PPP-AR, and Ginan, which were used to process GNSS data from both GPS-only and multi-GNSS (GPS, GLONASS, Galileo, BeiDou) constellations. The results indicate that PRIDE PPP-AR generally provided better horizontal and vertical positional accuracy than Ginan software, achieving improvements of up to approximately 33% in height component root mean square error (RMSE) for both constellation solutions. While the mean value of horizontal position differences for PRIDE PPP-AR in multi-GNSS solution was 4 cm, while 5 cm for Ginan. The anticipated advantages of multi-GNSS over GPS-only solutions were not consistently observed for Ginan software in 2D position and height components. However, PRIDE PPP-AR demonstrated improved internal consistency with multi-GNSS solution, achieving an RMSE value of 5 cm for horizontal positioning compared to 6 cm for Ginan. The general results of the study reveal that the PPP technique, which does not require any reference station's GNSS data, can achieve almost the same accuracy as the differential positioning technique. With this superiority, the PPP technique is an ideal positioning technique, especially in remote marine environments and polar regions, where geodetic infrastructure is inadequate and environmental conditions are difficult.

1. Introduction

Global Navigation Satellite Systems (GNSS) have revolutionized the field of geospatial positioning and navigation by providing accurate, reliable, and continuous 3D positioning. Among the various positioning techniques utilized in GNSS, the Precise Point Positioning (PPP) stands out by providing centimeter, even millimeter-level positioning accuracy using a single GNSS receiver without any base station data [1, 2]. Since Kouba and Heroux's first PPP solution in 2001 [2], the PPP technique has remained a widespread issue due to its economical and efficient nature, and academic research on the subject is ongoing.

The PPP technique leverages precise satellite orbit and clock corrections and biases data, often provided by various global institutions, including the International GNSS Service (IGS), the European Space Agency (ESA),

and the National Aeronautics and Space Administration (NASA). The quality and accuracy of these products are critical for PPP performance. For instance, IGS supplies precise orbit and clock products extensively utilized by the GNSS community for research and practical applications [3]. ESA's Navigation Support Office offers similar products focusing on European constellations, while NASA's Jet Propulsion Laboratory (JPL) provides precise products that support a wide range of scientific applications. Additionally, the IGS Multi-GNSS Experiment (MGEX) products play a crucial role in supporting multi-constellation GNSS research by providing precise orbit and clock products for emerging GNSS constellations including GLONASS, Galileo, and BeiDou in addition to GPS [4]. Multi-GNSS has significantly enhanced the robustness and accuracy of PPP solutions. Traditionally, the Global Positioning System (GPS) was the primary constellation used in PPP.

However, additional constellations have improved satellite availability and coverage, while enhancing the accuracy and reliability of PPP solutions [5-7]. Multi-GNSS has significantly enhanced the robustness and accuracy of PPP solutions. While the PPP technique does not directly contribute to minimizing multipath, the inclusion of multiple constellations provides additional independent observations, which improves the geometric strength and redundancy of the solution [8,9]. Observation redundancy in multi-GNSS strengthens the geometry and facilitates robust outlier detection. Signals suffered from multipath are then more readily down-weighted or excluded, reducing their overall impact on the final solution. This redundancy leads to better weighting of the observations and more effective detection of outliers, thus indirectly reducing the influence the effect of multipath [10].

Since the PPP technique was presented in the literature, many different PPP solution algorithms and software have been developed over the years and continue to be developed. One key advancement in this domain is the ability to fixed integer ambiguities, commonly referred to as PPP-AR, where phase biases are also handled. This approach significantly reduces the convergence time and improve the positioning accuracy compared to the traditional float ambiguity solution [11-15].

The PPP technique has been widely used in many fields like geodetic, atmospheric, and earth sciences [16-19]. This technique provides high accuracy depending on the processing algorithm used, the quality of the dataset, the observation time and conditions, the type of receiver, the used satellite system(s), and the frequencies. Previous static or kinematic PPP studies on land in the literature have demonstrated successful positioning performances in diverse environments [20,21]. However, relatively few studies carried out in marine or polar contexts [22,23]. It implies the necessity to further explore PPP performance under these conditions.

Dabove et al. [24] illustrated the advantages of multi-constellation PPP in high-latitude regions with harsh ionospheric scintillations, where convergence time and accuracy are critically affected. Furthermore, the integration of ambiguity fixed solution has improved convergence time and accuracy, making PPP a reliable tool even under geomagnetic disturbances [25]. Similarly, Ghoddousi-Fard et al. [26] explored the degradation of PPP under geomagnetic disturbances, emphasizing the necessity of robust algorithms for cycle slip detection and ambiguity resolution, particularly for high-latitude areas.

There are many scientific/academic, commercial, and open-source software and web-based services with unique features and advantages to obtain a 3D position in static/kinematic modes using the PPP technique whether real-time or post-processed with a float or fixed ambiguity solution. Brief information about these software types and services is given below.

- Scientific/Academic GNSS processing software, such as GipsyX, Bernese, and GAMIT/GLOBK, offer the opportunity to customize configurations. However, they

require deep GNSS knowledge, and some of them involve payments for licenses and even for updates [27-29].

- Commercial GNSS processing software, like CHCNAV Geomatics Office, Trimble Business Center, and GrafNav, offer high-precision positioning with robust support and user-friendly interfaces. On the other hand, these types of software do not offer users much choice in selecting the processing parameters compared to other types of software. Also, the high cost of such software is one of the known obstacles to their widespread use.

- The open-source in-house software generally does not have user-friendly interfaces and professional support sufficiently; however, they allow for greater flexibility and customization for researchers and appeal to advanced users who require more control over their processing parameters. Many open-source PPP software packages have been released in recent years, each with its own set of features and advantages. Examples include RTKLIB [30], GAMP [31], PPPH [32], PRIDE PPP-AR [33], MG-APP [34], PPPLib [35], SUPREME [36], raPPPid [37], and Ginan [38].

- Web-based online GNSS processing services, like APPS, CSRS-PPP, GAPS, magicGNSS, and Trimble CenterPoint RTX Post-Processing, provide an accessible platform for users who require accurate positioning without the need for software installation and maintenance. However, most of them are just capable of processing restricted combinations of constellations without parameter selection options [39,40].

Conducting kinematic GNSS measurements in Antarctica, and its inshore and offshore regions is challenging but crucial due to the unique challenges posed by the environment [41]. The high latitude results in lower satellite elevation angles, affecting signal quality and availability, which necessitates the use of multi-GNSS constellations to enhance satellite visibility and positioning accuracy [5]. In the Antarctic region, it is quite difficult to find a reference GNSS station at a close distance for high-accuracy static/kinematic 3D positioning with the GNSS relative positioning technique that provides the most accurate solution. In this region, there are no sufficiently dense reference GNSS stations. Moreover, most stations collect data only from GPS constellation, and it is quite difficult and costly to establish a new GNSS station. As a result, PPP—especially when utilizing multi-GNSS constellations—often becomes the most practical solution for achieving fast, cost-effective both static and kinematic solutions in these remote or extreme weather regions with insufficient geodetic and communication infrastructures [42]. It still provides sufficient accurate positioning, even if it is slightly lower than differential techniques as stated by Ebner and Featherstone [43] and Rizos et al. [44]. Reliable and accurate positioning is required for scientific research, marine surveying, navigation, and logistics operations in the Antarctic region, which is under the influence of harsh weather conditions. In marine areas, acquiring precise positioning is vital for safety and efficiency, enabling accurate navigation, timely response to changing conditions, and precise data collection. As mentioned by Bio et al. [45], the resolution and accuracy of bathymetric data are contingent upon

the quality of the sensing equipment, such as sonar, as well as the accuracy of GNSS positioning (± 10 cm). In addition, Shi et al. [46] demonstrated the capability to attain high positional accuracy, in the order of centimeters, through the use of the PPP technique, in their marine gravimetry study. Prominent studies have demonstrated the effectiveness of PPP at high latitudes, highlighting its potential to improve geodetic measurements and logistical operations in the region. The existing literature reveals that the real-time PPP solutions using the International GNSS Service (IGS) station data in the Antarctic region can produce 3D-position with centimeter-level accuracy [20,21,47]. Katsigianni et al. [48] assessed the accuracy of PPP and its phase ambiguity fixed resolution variant (PPP-AR) using Galileo-only, GPS-only, and multi-GNSS systems at CAS1 IGS station in Antarctica, revealing that the integration of Galileo with GPS leads to a significant improvement of about 30%, the accuracy founded as in 5 mm horizontal and 10 mm vertical for multi-GNSS PPP-AR. Bezcioglu et al. [22] conducted a comparative analysis of 3D-position derived from multi-GNSS PPP-AR and Double Difference (DD) techniques, utilizing kinematic measurements obtained from a boat). Their findings demonstrated that the post-processed PPP approach achieved a remarkable accuracy of 5.5 cm in the horizontal and 13.7 cm in the vertical component when employing the PPP-AR technique. These studies underscore the efficacy of PPP-AR in enhancing positional accuracy in dynamic environments such as marine navigation.

However, different software packages implement different strategies—such as employing various filter types (e.g., Kalman filter) or handling ambiguity resolution differently—and their performance may vary in different environmental conditions. Therefore, understanding the performance characteristics of each software is critical when operating in harsh surveying areas.

The main objective of this study is to conduct a usability and accuracy performance analysis of the multi-GNSS kinematic PPP technique in the polar region using data collected on a ship operating in the open-seas region of Antarctica. Another aim of the study is to determine whether multi-GNSS contributes to improving positioning accuracy compared to GPS-only solutions in these challenging conditions where satellite visibility is limited. To achieve the objectives of the study, we used the kinematic multi-GNSS observations collected on a research vessel moving from King George Island to Horseshoe Island, offshore in Antarctica continent. Additionally, this research investigates the impact of different open-source software packages on PPP accuracy, we therefore specifically utilized PRIDE PPP-AR and Ginan software, both of which are recognized for their capabilities in PPP, in this study [33,38]. PRIDE PPP-AR [33]—featuring advanced single-receiver ambiguity resolution—and Ginan [38], which incorporates a Kalman filter under a state-space representation. These two open-source tools represent complementary paradigms: a dedicated ambiguity-resolution approach versus dynamic filtering. By

evaluating their performance side by side, we aim to discover how each handles the challenges of high-latitude satellite geometry, harsh weather. Moreover, selecting appropriate processing tools for this study, we carefully considered both methodological diversity and practical applicability in polar environments. PRIDE PPP-AR's advanced ambiguity resolution technique is known to enhance positioning accuracy and significantly reduce convergence times, rendering it particularly effective various scenarios. Ginan, on the other hand, is a relatively new open-source software and its performance under extreme polar conditions has never been documented before. This study provides an opportunity to explore the potential of Ginan software in harsh environments, as the performance of this software has not yet been fully deciphered in polar or marine areas. We therefore chose a relatively new open-source software help fill that gap as well. By comparing these two complementary processing strategies—ambiguity fixed solutions versus dynamic filtering—we aim to provide insights into how different PPP methodologies address challenges while maintaining our work remains reproducible and accessible for future research.

The following section gives more detailed information about the dataset and processing results. This comprehensive analysis will provide valuable insights into the performance of multi-GNSS and the effectiveness of different PPP software in the Antarctic region, enhancing our understanding and capabilities in real-time positioning for both scientific and practical applications. It is seen that accurate and reliable 3D positioning is important in almost all scientific and other activities that are increasing day by day in this region, and the use of the PPP technique in these activities will provide a significant advantage. Although a limited number of studies have been done on this subject, it is evaluated that this study will make a significant contribution to filling an important gap in the literature.

2. Materials and Method

2.1. Data collection

In this study, a part of the kinematic multi-GNSS dataset collected during a 3-day cruise from King George Island to Horseshoe Island (750 km). within the scope of the 6th Turkish Antarctic Expedition 2022 was used. In the calculations, the 1Hz kinematic GNSS dataset collected on the ship, starting from about 01:00 PM to midnight on February 7, 2022 (GPS Day 38), was used.

The kinematic GNSS observations were carried out onboard the Betanzos, which is a research and survey ship with a Chilean flag. The 11-hour ship route used in the calculations, the reference PALM IGS station, as well as some main characteristics of the research vessel are given in Figure 1.

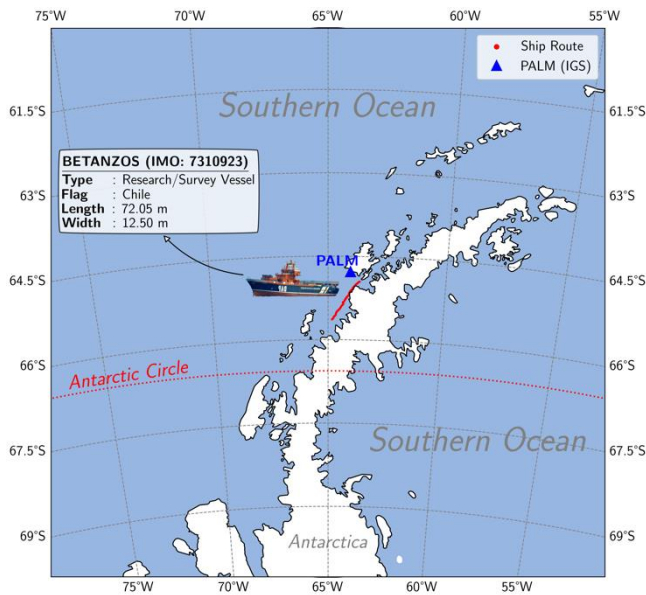


Figure 1. The ship route was used during the 6th Turkish Antarctic Expedition and the PALM IGS reference station.

During the cruise, the GNSS observations were collected using a CHCNAV i90 Pro Geodetic-grade GNSS receiver, capable of observing data with high precision and reliability. The CHC GNSS receiver offers multi-frequency capabilities, supporting multiple GNSS constellations, including GPS, GLONASS, Galileo, and BeiDou. It is equipped with advanced signal processing algorithms and provides robust performance even under adverse conditions, making it suitable for precise point positioning applications in harsh environments. Some specifications of the GNSS receiver used during the measurements are given in Table 1.

Table 1. Main specifications of the CHCNAV i90 Pro geodetic-grade GNSS receiver used in the study [49].

Item	Specifications
Frequencies	GPS : L1C, L1C/A, L2E, L2C, L5 GLONASS : L1C/A, L2C/A, L3 CDMA Galileo : E1, E5a, E5b, E5AltBOC, E6 BeiDou : B1, B2, B3 SBAS : L1C/A, L5 QZSS : L1C/A, L1SAIF, L2C, L5, LEX IRNSS : L5 L-BAND : RTX
Positioning rate	Up to 50 Hz
PPK accuracies	Horizontal : 2.5 mm + 1 ppm Vertical : 5 mm + 1 ppm
Data formats	HCN, HRC, RINEX 2.11, and 3.02
IP rate	IP67 waterproof
Environment	-40 °C to +65 °C

2.2. Data processing

To provide a comprehensive overview of the kinematic data, we present the skyplot of the tracked satellites during the observation period (Figure 2). The skyplot provides a visual representation of the satellites' positions relative to the observer, illustrating the distribution and coverage of GNSS satellites over time. When Figure 2 is investigated, it is understood that GPS, Galileo, and BeiDou satellites cannot be tracked in the zenith direction due to the orbital inclination of the systems, only GLONASS satellites can be tracked in this direction because of the 64.8-degree inclination orbit.

Figure 3 presents the time series view of the number of satellites (#SAT) available throughout the measurement period. The figure includes separate plots for GPS-only (G-only hereafter) and multi-GNSS (GREC, abbreviated hereafter as G (GPS), R (GLONASS), E (Galileo), and C (BeiDou) for each constellation, respectively) solutions. This visualization highlights the differences in satellite availability between the single-constellation and multi-constellation approaches over time.

The quality of the PPP solution is strongly influenced by the geometry of the satellites [50]. Both PRIDE PPP-AR and Ginan use an elevation-dependent stochastic model to account for the fact that low-elevation measurements are more sensitive to atmospheric errors [51]. In this approach, the noise variance of each observation is modeled as a function of the satellite's elevation angle typically using a relationship such as $\sigma^2 = \sigma_0^2 (1/\sin(\theta))^2$ where θ is the elevation angle. The stochastic model effectively down-weights observations from satellites at low elevations (e.g. those observed from the 180° azimuth), which are less reliable. In addition, the inclusion of GLONASS in the multi-GNSS configuration partially compensates for the reduced satellite geometry in the polar region by providing additional high elevation observations. It also contributes to mitigating the impact of poor geometry on the position estimates.

In order to demonstrate the advantages of GREC's geometric distribution compared to G-only, we also estimated the Dilution of Precision (DOP) values for two constellations, as horizontal (HDOP) and vertical (VDOP) dilution of precision. Figure 3 also includes HDOP and VDOP values, which were key indicators of the geometric strength of the satellite distribution and the potential accuracy of the positioning solution. In addition to Figure 3, the statistical information about these values are also given in Table 2.

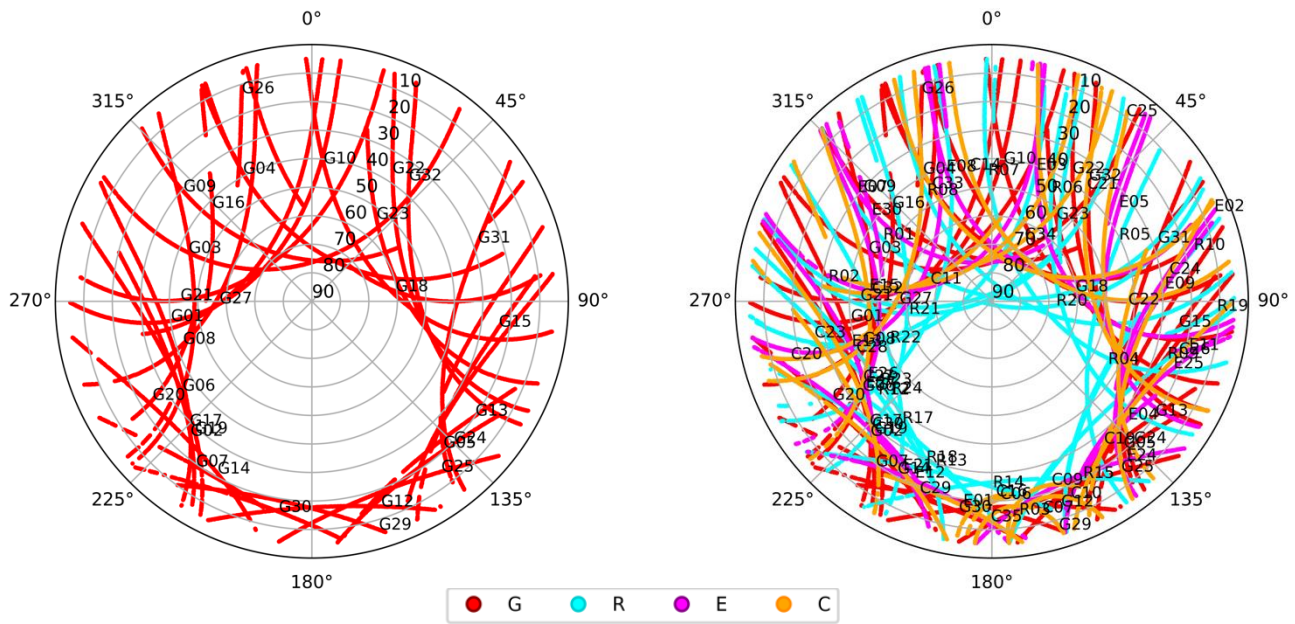


Figure 2. Skyplot of the tracked satellites throughout the measurement period for G-only (left) and GREC (right).

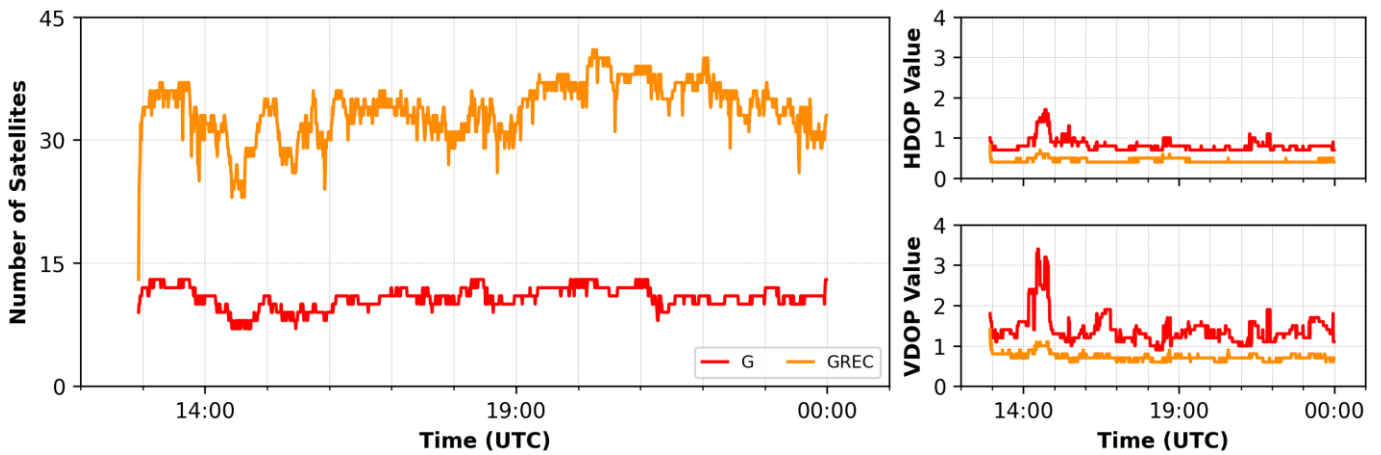


Figure 3. Number of satellites (#SAT), horizontal dilution of precision (HDOP), and vertical dilution of precision (VDOP) values over time.

Table 2. Statistical summary for number of satellites (#SAT), and dilution of precision (DOP) values for G-only and GREC constellations.

Constellation	Indicator	Min.	Max.	Mean
G-only	#SAT	7.0	13.0	11.0
	HDOP	0.7	1.7	0.8
	VDOP	0.9	3.4	1.4
GREC	#SAT	13.0	41.0	34.0
	HDOP	0.4	0.8	0.4
	VDOP	0.6	1.4	0.7

According to Figure 3 and Table 2, the average HDOP value was calculated as 0.8 for the G-only solution, whereas it was 0.4 for GREC. Similarly, the statistics with multi-GNSS combination improved the quality of VDOP from 1.4 to 0.7. The GREC combination has provided a 50% improvement in HDOP and VDOP values compared

to the G-only system. Similarly, while the average number of satellites observed in the G-only system is 11, the number reached 34 in the GREC combination, providing a 200% improvement.

As one of the signal quality indicators, signal-to-noise ratio (SNR) values related to the quality of the signals received from the observed satellites have also been calculated and are presented as skyplots for L1 and L2 frequencies in Figure 4. A greater SNR provides a more robust and reliable signal. In GNSS, an SNR value greater than a specified threshold (30-35 dBHz or above is generally accepted in various studies in the literature [52,53]) is regarded as proper for accurate positioning, whereas lower values may result in poor performance, particularly in challenging conditions with obstructions or interference.

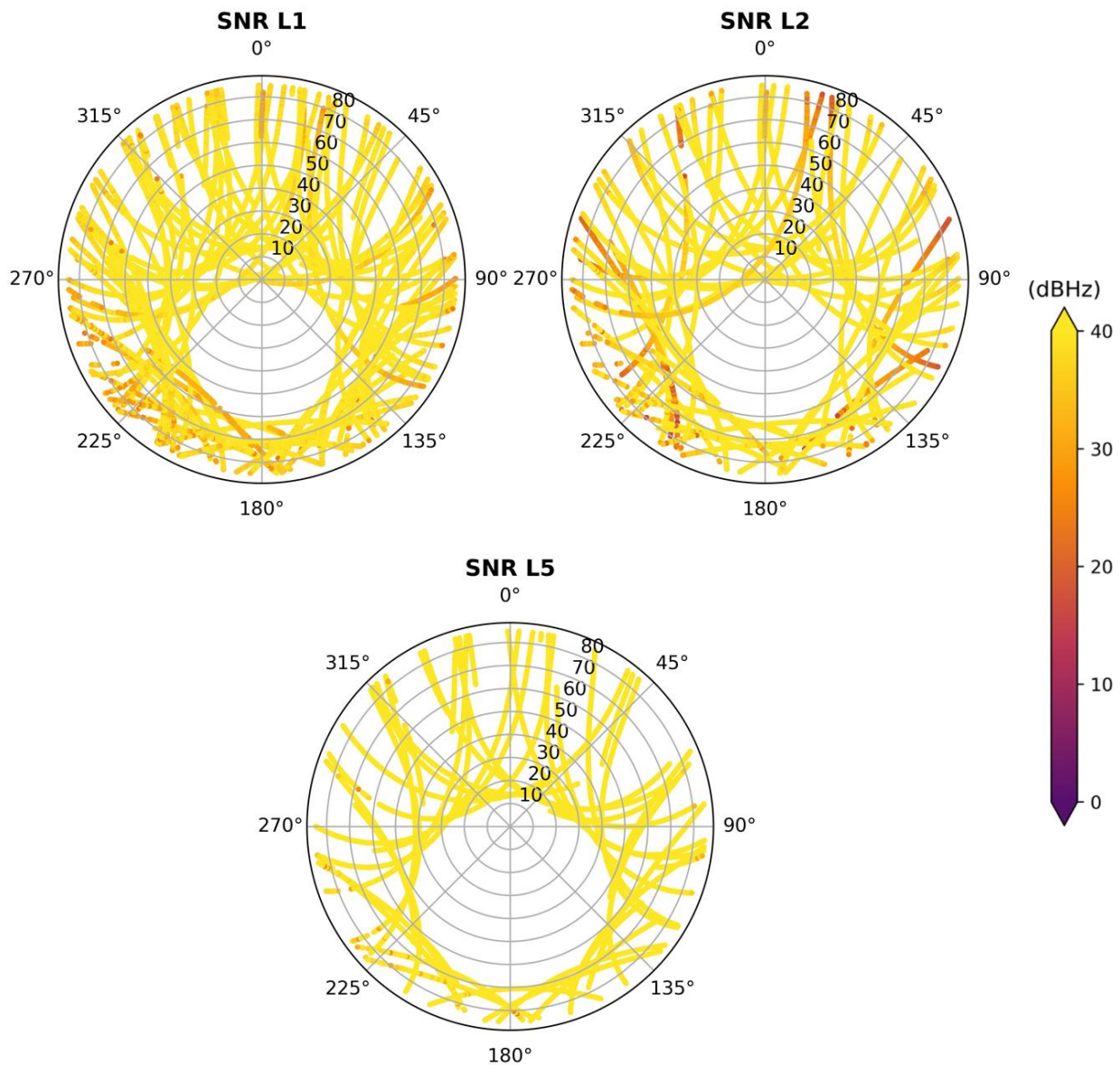


Figure 4. Skyplot of L1/E1 (left), L2 (right) and L5/E5 (bottom) frequency signal-to-noise ratio (SNR) values for the GREC constellation.

When Figure 4 is investigated, it can be seen that the L2 frequency contains more noise compared to the L1/E1, L5/E5 and that the SNR values of the data below a 20-degree elevation angle are lower than the values of the data with a high elevation angle, as expected from geodetic-grade GNSS antennas.

The coordinates obtained from relative positioning were used as known coordinates for each measurement epoch to assess the accuracy of the PPP-based coordinates. For this purpose, the collected kinematic data were processed using the conventional relative GNSS positioning technique, with the nearest station serving as the base station. Within the scope of this study, the PALM (64°46'30.3233" S, 64°3'4.0385" W), one of the stations of the International GNSS Service Network (IGS NET), was selected as a reference (Figure 1). To obtain the reference trajectory coordinates along the three-day route of the Betanzos ship, only the PALM IGS reference station with 1 Hz multi-GNSS data was found around the route. Unfortunately, no extra reference

station other than the PALM could be found to obtain 1Hz reference trajectory coordinates. Therefore, only the part of the whole data close to the PALM station was used in the calculations, with baseline lengths ranging from 27 km to 100 km. This relative positioning solution was carried out with CHCNV Geomatics Office Software 2.0 (CGO 2.0). The precise products released by the CODE (Center for Orbit Determination in Europe) Analysis Center under the MGEX project were used. Furthermore, the use of tropospheric model is crucial due to the long distances of the baselines, which is why the GPT2 climatological model and Vienna Mapping Function (VMF) 1 was employed as the tropospheric model for all baselines. In terms of the ionospheric model, the "Automatic Model" option within the software was employed, resulting in the computation of the ionospheric model using the L1 and L2 frequency combination.

By analyzing the dataset using two different software platforms, PRIDE PPP-AR (v3.0) and Ginan (v3.0.0), we

aim to evaluate the impact of multi-constellation GNSS on kinematic PPP results and quantify the performance of these software solutions in providing accurate absolute positioning in the extreme and dynamic conditions of the Antarctic region. PRIDE PPP-AR is an open-source software package developed by GNSS Research Center, Wuhan University. It is known for its advanced ambiguity resolution techniques, which enhance the accuracy of GNSS positioning by fixing integer ambiguities in the GNSS signal processing [33, 54]. It supports both static and kinematic solutions, making it versatile for various GNSS applications. It processes all-frequency signals on any dual-frequency. The software typically employs ionosphere-free combinations to mitigate ionospheric error, ensuring higher accuracy in positioning results, thus improving the robustness and reliability of positioning results. On the other hand, Ginan, an open-source GNSS processing software developed by Geoscience Australia, is designed for precise positioning services and supports a wide range of applications from geodetic research to practical navigation [38]. Ginan provides multi-GNSS solutions and incorporates advanced error modeling and correction techniques to enhance the accuracy and reliability of positioning solutions. One of the critical features of Ginan is its capability to deliver both real-time and post-processed positioning solutions, making it versatile for various applications in especially challenging environments like Antarctica. Additionally, Ginan employs enhanced Kalman Filtering to analyze GNSS data, improving the precision of the estimated positions by optimally filtering out noise and other errors [55]. Furthermore, these two software employ different techniques to detection and minimizing of noise. PRIDE PPP-AR uses a sequence of modules to identify suspicious epochs, detect cycle slips often triggered by strong multipath, and then exclude or re-weight observations with large post-fit residuals [33]. Ginan, on the other hand, adopts a Kalman Filter under a state-space representation to detect outliers. In high-multipath-error environments, Ginan's pre-processor checks geometry-free phase combinations, adjusts process noise in low-elevation observations, and discards satellites with excessively large residuals [38].

The 1Hz kinematic GNSS dataset used in the calculations was processed separately for both GPS-only and GREC constellations with PRIDE PPP-AR and Ginan software, and PPP-derived coordinates were obtained. Multi-GNSS precise products from CODE were utilized in both software applications during the process. To

provide a clear comparison between PRIDE PPP-AR and Ginan software, their main features are summarized in Table 3.

Table 3. Comparison of the features of PRIDE PPP-AR and Ginan software used in this study.

Feature	PRIDE PPP-AR (v3.0)	Ginan (v3.0.0)
Multi-GNSS Solution	Yes	Yes
Ambiguity Resolution	Fixed	Float
Real-Time (RT) Capability	No	Yes
Post-Processing (PP) Capability	Yes	Yes
Error Modeling and Corrections	Troposphere, Ionosphere, PCO*, PCV*, Phase wind-up, Tides, Relativity	
Adjustment Model	Batch Least-Square Processing	Kalman Filtering
Stochastic Model	Elevation Angle Dependent	
Troposphere	Saastamoinen model and GMF/VMF1/VMF3/NMF	
GNSS Constellations	Single constellation, All multi-GNSS combinations	Only GPS and GREC combination
Developed by	Wuhan University	Geoscience Australia
Main Applications	Research, Precise geodetic works	Geodetic research, Practical navigation

* PCO: Phase Center Offsets PCV: Phase Center Variations

3. Results

The PPP coordinates obtained with PRIDE PPP-AR and Ginan software using G-only and multi-GNSS (GREC) constellations were compared with the relative solution (known coordinates). The differences obtained for easting, northing (in UTM projection), 2D position, and ellipsoidal height components were given in Figure 5 for PRIDE-PPP and Figure 6 for Ginan software.

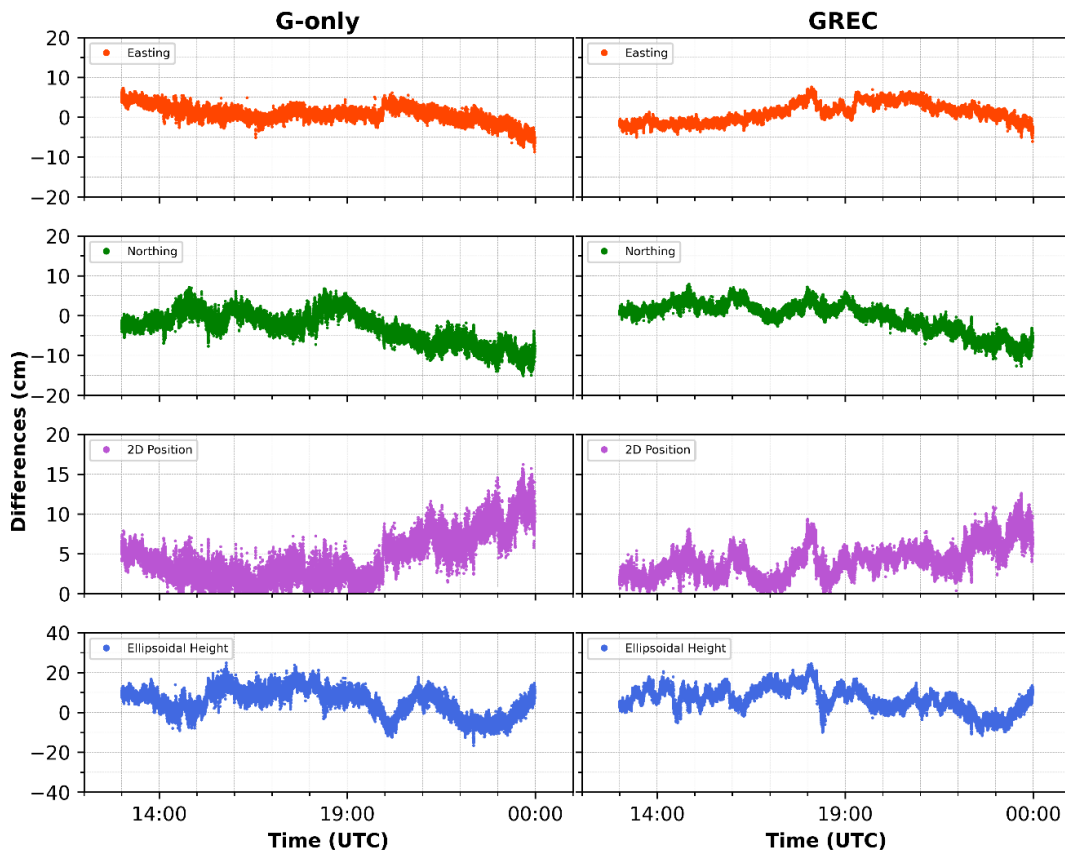


Figure 5. Time series of coordinate differences between PRIDE PPP-AR software solution and known coordinates for G-only (left) and GREC (right).

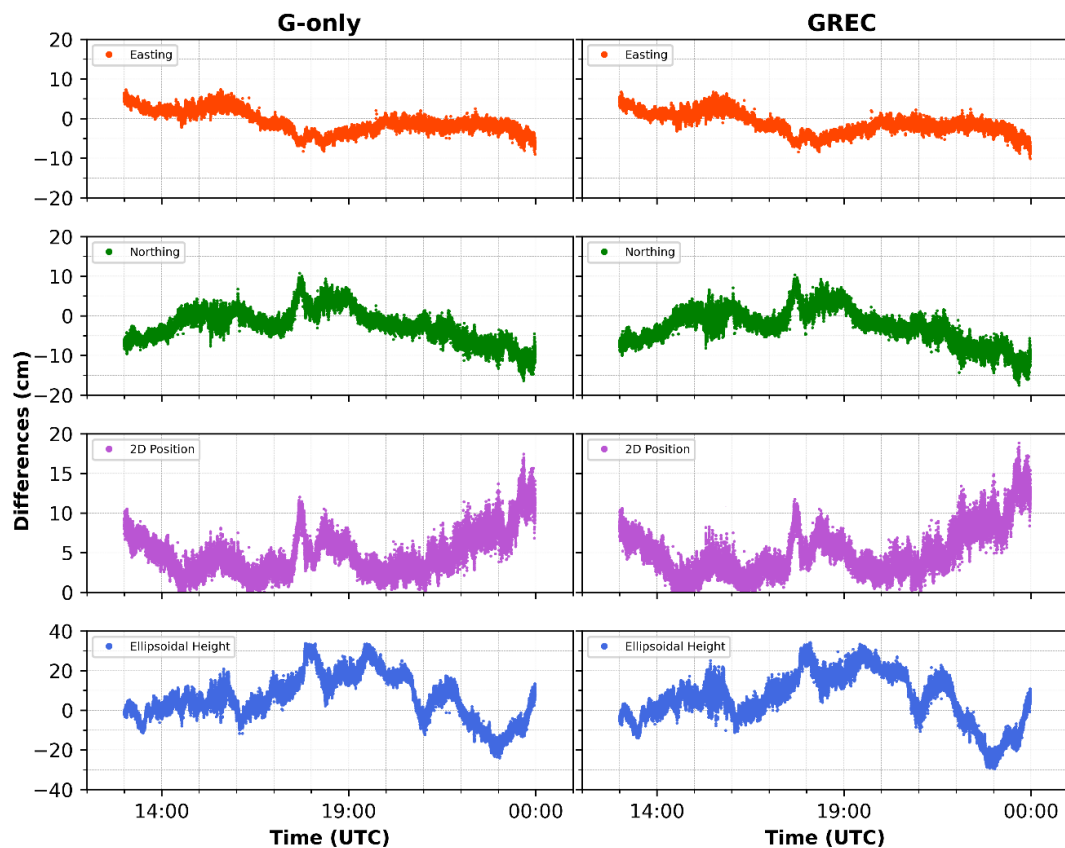


Figure 6. Time series of coordinate differences between Ginan software solution and known coordinates for G-only (left) and GREC (right).

The boxplot diagrams were also plotted in order to show the distribution of the obtained horizontal (2D) and vertical (h) position differences in Figure 7. A boxplot

graphically demonstrates the dataset's locality, spread, and skewness. The box in the middle shows the median (Q2), as well as the area between the first quartile (Q1)

and the third quartile (Q3), where 50% of the data is located, and is called the interquartile range (IQR). Q1 quartile represents the median of the data to the left side of the median (Q2) of the entire data, and Q3 represents the median of the data to the right side of Q2. The other 50% of the data is distributed to the right and left sides

of the box. Data outside the Q1-1.5IQR and Q3+1.5IQR whisker limits on the right and left of the box are outliers. The length of the box to the right and left relative to the median and the similarity of the data outside the box within itself indicate the skewness of the distribution.

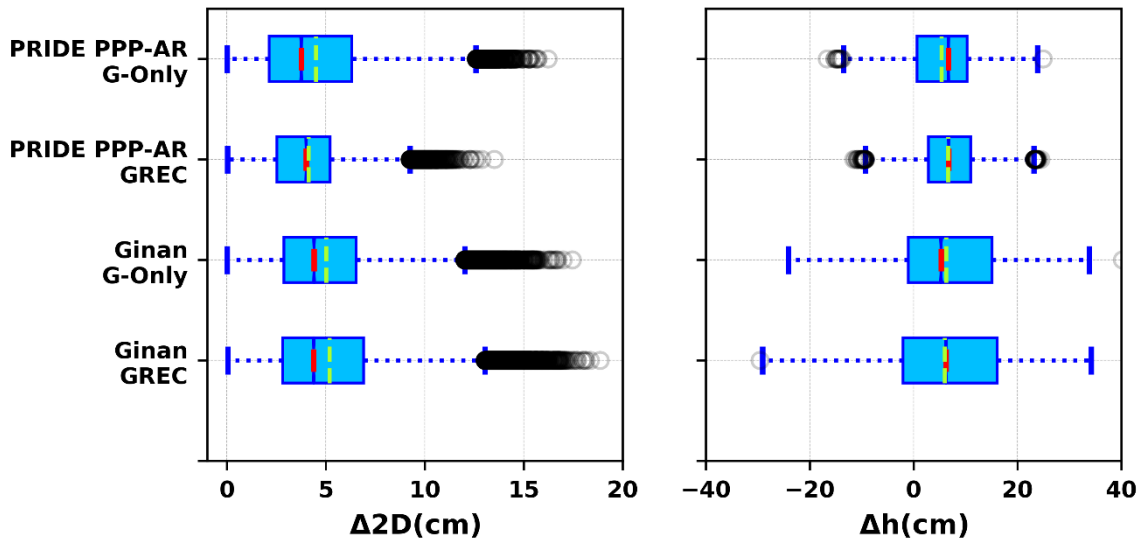


Figure 7. Boxplot graphs showing horizontal and vertical position differences for G-only and GREC solutions obtained from both PRIDE PPP-AR and Ginan software (the green line in the figure represents the mean, while the red line represents the median).

While presenting differences between the known coordinates and PPP solutions, we have defined the convergence time as the duration from the commencement of the process until the positional accuracy reaches below 20 cm for the 2D differences. It can be noted that both solutions yield the desired convergence time in a couple of minutes. Table 4 and 5 include the statistics of GPS-only and GREC 3D position components differences after convergence time for the two software.

Table 4. Statistical summary of position differences obtained using PRIDE PPP-AR solutions for G-only and GREC constellations.

Component	G-only				GREC			
	Min.	Max.	Mean	RMSE	Min.	Max.	Mean	RMSE
ΔE (cm)	-9	7	1	2	-6	8	1	3
ΔN (cm)	-15	7	-3	5	-13	8	0	4
Δ2D (cm)	0	16	5	5	0	14	4	5
Δh (cm)	-17	25	5	9	-12	25	7	9

Table 5. Statistical summary of position differences obtained using Ginan solutions for G-only and GREC constellations.

Component	G-only				GREC			
	Min.	Max.	Mean	RMSE	Min.	Max.	Mean	RMSE
ΔE (cm)	-9	7	-1	3	-10	7	-1	3
ΔN (cm)	-16	11	-2	5	-18	13	-3	5
Δ2D (cm)	0	17	5	6	0	19	5	6
Δh (cm)	-24	34	6	13	-30	34	6	14

When Figure 5, 6, and 7 are investigated, it is seen that the horizontal and height components of the G-only and GREC solutions obtained from both software have

positioning differences ranging from decimeters to centimeters. It is also seen that the horizontal position RMSE value of G-only and GREC solutions obtained from both software is below 1 decimeter, while the height component RMSE value is below 1 decimeter for PRIDE PPP-AR and above 1 decimeter for Ginan (see Table 4 and 5).

Examining the results presented in Table 4, Figures 5 and 7, it is observed that for the G-only solution, the 2D position difference reaches a maximum of 16 cm, with a 5 cm average and RMSE. For height component, the differences range from -17 to +25 cm, with an average value of 5 cm and an RMSE of 9 cm. In the GREC solution, the 2D position difference has a maximum of 14 cm, with an average of 4 cm and an RMSE of 5 cm. On the other hand, height differences range between -12 and +25 cm, with an average of 7 cm and an RMSE of 9 cm. Although numerically it appears that the 2D position and height differences, together with their accuracies, obtained by the PRIDE PPP-AR, remain unchanged with multi-GNSS, the difference graphs in Figure 5 and the boxplots in Figure 7 show that the multi-GNSS results have become more internally consistent, despite the existence of some outliers. When analyzing the differences, distributions, and statistics of Ginan solutions given in Figures 6, 7, and Table 5, reveals different results compared to the PRIDE PPP-AR solutions. According to the Ginan results, multi-GNSS solutions do not provide significant numerical improvements for 2D and height differences, or RMSE values. In the Ginan G-only solution, the 2D position difference has a maximum of 17 cm, with an average of 5 cm and an RMSE of 6 cm. Height differences are between -24 and +34 cm, with an average value of 6 cm and an RMSE of 13 cm. In the Ginan GREC solution, the 2D

position difference has a maximum of 19 cm, with an average of 5 cm and an RMSE of 6 cm. For height differences range between -30 and +34 cm, with an average of 6 cm and an RMSE of 14 cm. It implies that the GREC solution obtained with the Ginan software offers no improvements in horizontal or vertical positioning compared to the G-only solution. Similarly, the Ginan boxplots in Figure 7 do not show a significant advantage of the multi-GNSS solution over the G-only solution.

Comparing Table 4 and Table 5, it is implied that for both G-only and GREC solutions, the PRIDE PPP-AR software improves the accuracy of the height component by approximately 33% compared to the Ginan software (reducing from 13 cm to 9 cm for the G-only and from 14 cm to 9 cm for the multi-GNSS solution).

The analysis further reveals that the PRIDE PPP-AR solution produces slightly better horizontal and vertical RMSE compared to Ginan for both G-only and GREC configurations (Tables 4 and 5). This may be interpreted as PRIDE PPP-AR's advanced ambiguity resolution techniques contributing to more accurate positioning solutions [56,57].

While PRIDE PPP-AR demonstrates relatively better performance compared to Ginan, the anticipated benefits of multi-GNSS over G-only solutions are not uniformly observed. One possible reason may be the weighting criteria differences among different satellite systems for each software. This detailed comparison between the PRIDE PPP-AR and Ginan solutions underscores the importance of using advanced software for precise positioning but also highlights the complexity of achieving consistent improvements using solely multi-GNSS configurations for kinematic GNSS observation.

4. Conclusion

This study set out to evaluate the performance of the G-only and multi-constellation GNSS PPP technique for offshore kinematic applications in the challenging environment of Antarctica. In polar regions, since satellites cannot be observed in the zenith direction due to GNSS satellite orbit inclination angle, it is important to use GLONASS satellites with higher orbit inclination angle in short-term measurements. Therefore, in this study, the GREC solution was implemented with two different PPP software, and its advantages compared to the G-only solution were investigated. Although web-based PPP services are easier to use, the fact that these services do not have quad-GNSS or multi-frequency support and do not allow users to choose processing parameters has paved the way for the use of open-source (in-house) software (i.e. PRIDE PPP-AR and Ginan) that provide more flexibility to the user in many academic and practical studies. The findings of the study indicate that PRIDE PPP-AR software has relatively better results overall compared to Ginan software in both G-only and GREC configurations. Furthermore, in the kinematic PPP solution, while Ginan cannot reveal the contribution of GREC configuration compared to the G-only solution, PRIDE PPP-AR software has advantages on this subject with its advanced ambiguity resolution algorithm. It should be noted that the use of the PPP technique instead of the relative positioning technique has advanced

contributions, especially in regions that are not suitable for the establishment of dense GNSS networks and open-seas. To obtain the reference coordinates required to validate the PPP solutions, the relative positioning solution and therefore at least one reference GNSS station at a close distance to the study area are needed. In this study, no reference stations were found that fit the entire 3-day ship route, and only the PALM IGS station could be found in the region that fit the 2nd day of the ship route. It is quite difficult to find a proper reference station at a sufficient distance to obtain a relative solution in the Antarctic region, which necessitates the use of the PPP technique in the area. The horizontal and vertical accuracies obtained by both software solutions for both satellite configurations indicate that the PPP technique is sufficiently suitable for many marine applications. Despite the challenges posed by the Antarctic environment, achieving a positional accuracy of less than one decimeter is still notable for kinematic GNSS observations in maritime settings [45,46]. According to the accuracy levels obtained from the study, this level of accuracy is useful and sufficient for many positioning applications [58-61], like earth and marine sciences, precise hydrographic surveys, mapping, and logistics, in polar regions [20-23].

Acknowledgement

This study was carried out under the auspices of the Presidency of the Republic of Turkey, supported by the Ministry of Industry and Technology, and coordinated by TUBITAK MAM Polar Research Institute.

Author contributions

Volkan Özbey: Investigation, Conceptualization, Methodology, Writing-Original draft preparation
Bilal Mutlu: Visualization, Conceptualization, Data curation, Software, Writing-Original draft preparation
Serdar Erol: Investigation, Conceptualization, Methodology, Writing-Reviewing and Editing
Mahmut Oğuz Selbesoğlu: Field study, Reviewing and Editing
Hasan Hakan Yavaşoğlu: Field study
Reha Metin Alkan: Conceptualization, Methodology, Writing-Reviewing and Editing, Supervision.

Conflicts of interest

The authors declare no conflicts of interest.

References

1. Zumberge, J. F., Heflin, M. B., Jefferson, D. C., Watkins, M. M., & Webb, F. H. (1997). Precise point positioning for the efficient and robust analysis of GPS data from large networks. *Journal of Geophysical Research: Solid Earth*, 102(B3), 5005–5017.
2. Héroux, P., & Kouba, J. (2001). GPS precise point positioning using IGS orbit products. *Physics and Chemistry of the Earth, Part A: Solid Earth and Geodesy*, 26(6–8), 573–578.
3. Dow, J. M., Neilan, R. E., & Rizos, C. (2009). The International GNSS Service in a changing landscape of

- Global Navigation Satellite Systems. *Journal of Geodesy*, 83(3-4), 191-198.
4. Rizos, C., Montenbruck, O., Weber, R., Weber, G., Neilan, R., & Hugentobler, U. (2013). The IGS MGEX experiment as a milestone for a comprehensive multi-GNSS service. *Proceedings of the ION 2013 Pacific PNT Meeting*, 289-295, Honolulu, Hawaii.
 5. Montenbruck, O., Steigenberger, P., & Hauschild, A. (2018). Multi-GNSS signal-in-space range error assessment – Methodology and results. *Advances in Space Research*, 61(12), 3020-3038.
 6. Ögütçü, S., Shakor, A., & Farhan, H. (2022). Investigating the effect of observation interval on GPS, GLONASS, Galileo and BeiDou static PPP. *International Journal of Engineering and Geosciences*, 7(3), 294-301.
 7. Uçarlı, A. C., Demir, F., Erol, S., & Alkan, R. M. (2021). Farklı GNSS Uydu Sistemlerinin Hassas Nokta Konumlama (PPP) Tekniğinin Performansına Etkisinin İncelenmesi. *Geomatik*, 6(3), 247-258.
 8. Zheng, K., Zhang, X., Li, P., Li, X., Ge, M., Guo, F., Sang, J., & Schuh, H. (2019). Multipath extraction and mitigation for high-rate multi-GNSS precise point positioning. *Journal of Geodesy*, 93, 2037-2051.
 9. Zheng, K., Tan, L., Liu, K., Chen, M., & Zeng, X. (2023). Assessing the Performance of Multipath Mitigation for Multi-GNSS Precise Point Positioning Ambiguity Resolution. *Remote Sensing*, 15(17), 4137.
 10. Bu, J., Yu, K., Qian, N., Zuo, X., & Chang, J. (2021). Performance assessment of positioning based on multi-frequency multi-GNSS observations: signal quality, PPP and baseline solution. *IEEE Access*, 9, 5845-5861.
 11. Loyer, S., Perosanz, F., Mercier, F., Capdeville, H., & Marty, J. C. (2012). Zero-difference GPS ambiguity resolution at CNES-CLS IGS Analysis Center. *Journal of Geodesy*, 86, 991-1003.
 12. Pan, L., Xiaohong, Z., & Fei, G. (2017). Ambiguity resolved precise point positioning with GPS and BeiDou. *Journal of Geodesy*, 91, 25-40.
 13. Li, X., Li, X., Yuan, Y., Zhang, K., Zhang, X., & Wickert, J. (2018). Multi-GNSS phase delay estimation and PPP ambiguity resolution: GPS, BDS, GLONASS, Galileo. *Journal of Geodesy*, 92, 579-608.
 14. Ögütçü, S. (2020). Performance analysis of ambiguity resolution on PPP and relative positioning techniques: consideration of satellite geometry. *International Journal of Engineering and Geosciences*, 5(2), 73-93.
 15. Bezcioglu, M., Uçar, T., & Yiğit, C. Ö. (2023). Investigation of the capability of multi-GNSS PPP-AR method in detecting permanent displacements. *International Journal of Engineering and Geosciences*, 8(3), 251-261.
 16. Alkan, R. M., Erol, S., İlçi, V., & Ozulu, İ. M. (2020). Comparative analysis of real-time kinematic and PPP techniques in dynamic environment. *Measurement*, 163, 107995.
 17. Yiğit, C. O., El-Mowafy, A., Anil Dindar, A., Bezcioglu, M., & Tiryakioğlu, I. (2021). Investigating performance of high-rate GNSS-PPP and PPP-AR for structural health monitoring: dynamic tests on shake table. *Journal of Surveying Engineering*, 147(1).
 18. Vana, S., & Bisnath, S. (2023). Low-cost, triple-frequency, multi-GNSS PPP and MEMS IMU integration for continuous navigation in simulated urban environments. *NAVIGATION: Journal of the Institute of Navigation*, 70(2), navi.578.
 19. Pan, L., Deng, M., & Chen, B. (2024). Real-time GNSS meteorology: a promising alternative using real-time PPP technique based on broadcast ephemerides and the open service of Galileo. *GPS Solutions*, 28(3), 113.
 20. Alkan, R. M., Erol, S., & Mutlu, B. (2023). Applicability of real-time PPP technique in polar regions as an accurate and efficient real-time positioning system. *Turkish Journal of Earth Sciences*, 32(8), 1022-1040.
 21. Erol, S., Alkan, R. M., & Mutlu, B. (2023). Assessment of multi-GNSS RT-PPP services for the Antarctic region. *Arctic*, 76(3), 357-369.
 22. Bezcioglu, M., Yigit, C. O., & El-Mowafy, A. (2019). Kinematic PPP-AR in Antarctic comparing methods for precise positioning. *Sea Technology*, 60(2), 20-23.
 23. Alkan, R. M., Selbesoğlu, M. O., Yavaşoğlu, H. H., & Arkalı, M. (2024). Seamless precise kinematic positioning in the high-latitude environments: Case study in the Antarctic Region. *Rudarsko-Geološko-Naftni Zbornik*, 39(2), 31-43.
 24. Dabove, P., Linty, N., & Doyis, F. (2020). Analysis of multi-constellation GNSS PPP solutions under phase scintillations at high latitudes. *Applied Geomatics*, 12, 45-52.
 25. Luo, X., Chen, Z., Gu, S., Yue, N., & Yue, T. (2023). Studying the fixing rate of GPS PPP ambiguity resolution under different geomagnetic storm intensities. *Space Weather*, 21(10), e2023SW003542.
 26. Ghoddousi-Fard, R., & Lahaye, F. (2015). High latitude ionospheric disturbances: Characterization and effects on GNSS precise point positioning. *Proceedings of the 2015 International Association of Institutes of Navigation World Congress (IAIN)*, 1-6, Prague, Czech Republic.
 27. Bertiger, W., Bar-Sever, Y., Dorsey, A., Haines, B., Harvey, N., Hemberger, D., ... & Willis, P. (2020). GipsyX/RTGx, a new tool set for space geodetic operations and research. *Advances in space research*, 66(3), 469-489.
 28. Herring, T. A., King, R. W., & McClusky, S. C. (2010). *Introduction to gamit/globk*. Massachusetts Institute of Technology, Cambridge, Massachusetts.
 29. Dach, R., & Arnold, D. (2025). *Bernese GNSS Software Version 5.4 Tutorial*. Astronomical Institute, University of Bern, Bern, Switzerland.
 30. Takasu, T. (2010). Real-time PPP with RTKLIB and IGS real-time satellite orbit and clock. *IGS Workshop 2010*, Newcastle upon Tyne, England.
 31. Zhou, F., Dong, D., Li, W., Jiang, X., Wickert, J., & Schuh, H. (2018). GAMP: An open-source software of multi-GNSS precise point positioning using undifferenced and uncombined observations. *GPS Solutions*, 22(2), 33.
 32. Bahadur, B., & Nohutcu, M. (2018). PPPH: a MATLAB-based software for multi-GNSS precise point positioning analysis. *GPS Solutions*, 22(4), 113.

33. Geng, J., Chen, X., Pan, Y., Mao, S., Li, C., Zhou, J., & Zhang, K. (2019). PRIDE PPP-AR: an open-source software for GPS PPP ambiguity resolution. *GPS Solutions*, 23(4), 91.
34. Xiao, G., Liu, G., Ou, J., Liu, G., Wang, S., & Guo, A. (2020). MG-APP: an open-source software for multi-GNSS precise point positioning and application analysis. *GPS Solutions*, 24(3), 66.
35. Chen, C., & Chang, G. (2021). PPPLib: An open-source software for precise point positioning using GPS, BeiDou, Galileo, GLONASS, and QZSS with multi-frequency observations. *GPS Solutions*, 25(1), 18.
36. Zhao, C., Zhang, B., & Zhang, X. (2021). SUPREME: an open-source single-frequency uncombined precise point positioning software. *GPS Solutions*, 25(3), 86.
37. Glaner, M. F., & Weber, R. (2023). An open-source software package for precise point positioning: raPPPid. *GPS Solutions*, 27(4), 174.
38. McClusky, S., Hammond, A., Maj, R., Allgeyer, S., Harima, K., Yeo, M., ... & Riddell, A. (2024). Precise point positioning with Ginan: Geoscience Australia's open-source GNSS analysis centre software. *Proceedings of the ION 2024 Pacific PNT Meeting*, 248–280, Honolulu, Hawaii.
39. Pırtı, A., & Yazıcı, D. (2022). İnternet tabanlı GNSS yazılımlarının doğruluk açısından değerlendirilmesi. *Geomatik*, 7(2), 88-105.
40. Özdemir, E. G. (2022). Bağıl ve mutlak (PPP) konum çözüm yaklaşımı sunan Web-Tabanlı çevrimiçi veri değerlendirme servislerinin farklı gözlem periyotlarındaki performanslarının araştırılması. *Geomatik*, 7(1), 41-51.
41. Li, X., Huang, J., Li, X., Shen, Z., Han, J., Li, L., & Wang, B. (2022). Review of PPP-RTK: Achievements, challenges, and opportunities. *Satellite Navigation*, 3(1), 28.
42. Di, M., Guo, B., Ren, J., Wu, X., Zhang, Z., Liu, Y., Liu, Q., & Zhang, A. (2022). GNSS Real-Time Precise Point Positioning in Arctic Northeast Passage. *Journal of Marine Science and Engineering*, 10(10), 1345.
43. Ebner, R., & Featherstone, W. (2008). How well can online GPS PPP post-processing services be used to establish geodetic survey control networks? *Journal of Applied Geodesy*, 2(3), 149-157.
44. Rizos, C., Janssen, V., Roberts, C., & Grinter, T. (2012). Precise Point Positioning: Is the Era of Differential GNSS Positioning Drawing to an End? *FIG Working Week 2012: Knowing to manage the territory, protect the environment, evaluate the cultural heritage*, Rome, Italy.
45. Bio, A., Gonçalves, J.A., Magalhães, A., Pinheiro, J., & Bastos, L. (2022). Combining low-cost sonar and high-precision global navigation satellite system for shallow water bathymetry. *Estuaries and Coasts*, 45, 1000-1011.
46. Shi, Z., Lang, J., Liang, X., Zhou, Z., Guo, A., & Liu, L. (2021). Experimental study on improving the accuracy of marine gravimetry by combining moving-base gravimeters with GNSS antenna array. *Earth Planets Space*, 73, 174.
47. Alkan, R. M., Erol, S., & Mutlu, B. (2022). IGS-RTS ürünleri kullanılarak gerçek-zamanlı hassas nokta konumlama (RT-PPP) tekniğinin performans analizi: Antarktika örneği. *Yerbilimleri*, 43(1), 76-95.
48. Katsigianni, G., Loyer, S., & Perosanz, F. (2019). PPP and PPP-AR Kinematic Post-Processed Performance of GPS-Only, Galileo-Only and Multi-GNSS. *Remote Sensing*, 11(21), 2477.
49. Shanghai Huace Navigation Technology (CHCNAV) Ltd. (2021). CHCNAV i90 Pro IMU-RTK receiver user guide. Shanghai, China.
50. Montenbruck, O., Schmid, R., Mercier, F., Steigenberger, P., Noll, C., Fatkulin, R., ... & Ganeshan, A. S. (2015). GNSS satellite geometry and attitude models. *Advances in Space Research*, 56(6), 1015-1029.
51. Hofmann-Wellenhof, B., Lichtenegger, H., & Wasle, E. (2007). *GNSS—global navigation satellite systems: GPS, GLONASS, Galileo, and more*. Springer Science & Business Media.
52. Abidin, W. A. W. Z., Fujisaki, K. & Tateiba, M. (2008). Novel approach to determine the effects of MS environment using the portable GPS receiver with built-in antenna. *American Journal of Applied Sciences*, 5(8), 1079-1082.
53. Lau, L., & Mok, E. (1999). Improvement of GPS relative positioning accuracy by using SNR. *Journal of surveying engineering*, 125(4), 185-202.
54. Geng, J., Yang, S., & Guo, J. (2021). Assessing IGS GPS/Galileo/BDS-2/BDS-3 phase bias products with PRIDE PPP-AR. *Satellite Navigation*, 2(1), 17.
55. Strandberg, J., Hobiger, T., & Haas, R. (2019). Real-time sea-level monitoring using Kalman filtering of GNSS-R data. *GPS Solutions*, 23(3), 61.
56. Geng, J., Meng, X., Dodson, A. H., & Teferle, F. N. (2010). Integer ambiguity resolution in precise point positioning: method comparison. *Journal of Geodesy*, 84(9), 569-581.
57. Zhang, X., Zhang, Y., & Zhu, F. (2020). A method of improving ambiguity fixing rate for post-processing kinematic GNSS data. *Satellite Navigation*, 1(1), 20.
58. Karadeniz, B., Pehlivan, H., & Arı, B. (2023). Examination of the Performance of Precise Point Positioning Technique with Real-Time Products on Smartphones. *Advanced Geomatics*, 3(1), 33-39.
59. Karadeniz, B., Pehlivan, H., Altıntaş, A. F., & Usta, S. (2024). Comparison of Network-RTK and PPP Technique in terms of Position Accuracy. *Advanced Geomatics*, 4(1), 31-36.
60. Demez, B., & Ernst, F. B. (2024). Creating Climate Change Scenarios Using Geodesing Method: Pütürge District Example. *Advanced Geomatics*, 4(1), 01-08.
61. Balci, D. (2022). Researching the use of infrastructure in land management. *Advanced GIS*, 2(1), 18-23.

